Bioactives of *Artemisia dracunculus L.* Mitigate the Role of Ceramides in Attenuating Insulin Signaling in Rat Skeletal Muscle Cells

Diana N. Obanda,[1] Amy Hernandez,[2] David Ribnicky,[1,3] Yongmei Yu,[1] Xian H. Zhang,[1] Zhong Q. Wang,[1] and William T. Cefalu[1]

Ectopic lipids in peripheral tissues have been implicated in attenuating insulin action in vivo. The botanical extract of *Artemisia dracunculus L.* (PMI 5011) improves insulin action, yet the precise mechanism is not known. We sought to determine whether the mechanism by which PMI 5011 improves insulin signaling is through regulation of lipid metabolism. After differentiation, cells were separately preincubated with free fatty acids (FFAs) and ceramide C2, and the effects on glycogen content, insulin signaling, and ceramide profiles were determined. The effect of PMI 5011 on ceramide accumulation and ceramide-induced inhibition of insulin signaling was evaluated. FFAs resulted in increased levels of total ceramides and ceramide species in L6 myotubes. Saturated FFAs and ceramide C2 inhibited insulin-stimulated phosphorylation of protein kinase B/Akt and reduced glycogen content. PMI 5011 had no effect on ceramide formation or accumulation but increased insulin sensitivity via restoration of Akt phosphorylation. PMI 5011 also attenuated the FFA-induced upregulation of a negative inhibitor of insulin signaling, i.e., protein tyrosine phosphatase 1B (PTP1B), and increased phosphorylation of PTP1B. PMI 5011 attenuates the reduction in insulin signaling induced by ceramide accumulation, but the mechanism of improved insulin signaling is independent of ceramide formation. ***Diabetes*** **61:597–605, 2012**

Insulin resistance is a major pathophysiologic parameter characterizing obesity and type 2 diabetes (T2DM). Because skeletal muscle is the major target tissue for insulin action, skeletal muscle insulin resistance is a major contributor to reduced whole-body glucose disposal in obesity and T2DM. In addition, there is a strong correlation between insulin resistance and lipid accumulation in tissues, i.e., ectopic lipids. This condition typically develops in association with weight gain, prolonged physical inactivity, and/or systemic hyperlipidemia (1). In this regard, both in vitro and in vivo studies have demonstrated that exposure of muscle to excessive lipids leads to accumulation of fatty acid–derived metabolites such as triacylglycerols, diacylglycerols, and ceramides. These lipid metabolites are reported to initiate pathways leading to the inactivation of various insulin signaling intermediates (1–4). Elevated ceramide levels in particular have been suggested in a number of pathological states including inflammation, cancer, obesity, insulin resistance, and T2DM (5–7) and inhibit a number of kinases that are stimulated by insulin, including protein kinase B (PKB/Akt) and protein kinase C (5).

Interventions that improve insulin sensitivity have been suggested to lower muscle ceramide levels. Specifically, insulin sensitizing agents such as thiazolidinediones, in addition to exercise, have been shown to dramatically lower muscle ceramide levels in both humans and rodents (4,8–10). These studies suggest that therapeutic interventions aimed at reducing lipid intermediates in vivo in general, and ceramide levels in particular, could be a useful therapeutic strategy for the treatment of insulin resistance. Unfortunately, current available agents used to treat insulin resistance have been associated with significant adverse effects. As such, there has been a search for safe and effective alternative therapies. In this regard, plants have traditionally been a rich source of medicinal compounds for many indications, including diabetes, and there are a number of reports about the use of plants from the genus Artemisia as a traditional treatment for diabetes. Specifically, *Artemisia dracunculus L.* or Russian tarragon is a perennial herb with a long history of medicinal and culinary use. The ethanolic extract of *A dracunculus L.* (PMI 5011) has been shown to significantly decrease blood glucose levels in both genetic and chemically induced murine models of diabetes and improve insulin action (11–14). We hypothesized that PMI 5011 improves insulin sensitivity by lowering intramuscular lipid intermediates. To accomplish our objectives, we used tandem mass spectrometry and sought to investigate whether the mechanism by which PMI 5011 improves insulin signaling is secondary to modulation of cellular lipid metabolism with respect to ceramide formation and action.

RESEARCH DESIGN AND METHODS

Source and characterization of PMI 5011. PMI 5011 was produced from plants grown hydroponically under uniform and controlled conditions, thereby standardizing phytochemical content. The growing, quality control, biochemical characterization, and preparation of PMI 5011 have been reported (11–14). For this study, PMI 5011 was evaluated at 10 μg/mL, a dose determined to be the lowest most effective level from previous studies (12–14).

Standards and reagents. Ceramide standards and reagents were purchased from Avanti Polar Lipids (Alabaster, AL). All organic solvents were of high-performance liquid chromatography grade, American Chemical Society certified. Myriocin and free fatty acids (FFAs) were obtained from Sigma-Aldrich. The plasmid pMko.1 puro PTEN short hairpin RNA was obtained from Addgene.

Cell culture. L6 myoblasts were obtained from the American Type Culture Collection and maintained at 37°C, 95% air, and 5% CO_2 in low glucose Dulbecco's modified Eagle's medium supplemented with 10% CBS serum and antibiotics. For individual experiments, myoblasts were subcultured onto 6 or 12 well plates, grown to 80–90% confluence, and differentiated into fused

From the [1]Botanical Research Center, Pennington Biomedical Research Center, Louisiana State University System, Baton Rouge, Louisiana; the [2]Department of Agricultural Chemistry, Louisiana State University System, Baton Rouge, Louisiana; and the [3]Biotech Center, Rutgers University, New Brunswick, New Jersey.

Corresponding author: William T. Cefalu, William.Cefalu@pbrc.edu.

Received 24 March 2011 and accepted 9 December 2011.

DOI: 10.2337/db11-0396

This article contains Supplementary Data online at http://diabetes.diabetesjournals.org/lookup/suppl/doi:10.2337/db11-0396/-/DC1.

myotubes for 5 days by switching to media with 2% horse serum. All cells used were within five passages.

FFA and ceramide treatment. Cultures were exposed to FFAs conjugated with 1% BSA and constituted to a final concentration 200 μM or ceramide C2 in DMSO at 20 or 40 ng/mL. For insulin signaling studies, myotubes were serum-starved in Dulbecco's modified Eagle's media containing 0.2% BSA and treated with FFAs or ceramide C2 for 16 h. Insulin was added at a final concentration of 100 nmol/L for 5 min before subsequent analysis.

Glycogen content. Glycogen content in basal and insulin stimulated states was assessed on cells grown in 12 well plates with use of glycogen hydrolysis and glucose determination according to the method of Gómez-Lechón et al. (15) with modifications shown in Wang et al. (13). Results were normalized by protein concentration measured by Bio-Rad protein assay kit (Bio-Rad Laboratories, Hercules, CA), and glycogen content was presented as micrograms glucose equivalent per well.

Lipid extraction. Cells grown in 6 well plates were collected with 200 μL ice-cold deionized water after 24 h incubation with FFAs with or without PMI 5011. After sonication, 2 μL was removed for protein concentration measurement. An aliquot equivalent to 300 μg protein was extracted according to the method of Haynes et al. (16) with modifications. In brief, 4 μL of a 10 μg/mL ceramide C17 solution were added as the extraction standard. Lipids were extracted with 500 μL of methanol/chloroform (1:2). The suspension was vortexed and placed on a shaker at 4°C for 1 h. Lysates were spun (10 min, 10,000 rpm). The lower chloroformic layer was transferred to a new tube and placed on ice. The upper methanolic and the middle proteinous layers were sonicated and subjected to a second extraction. The lower chloroformic layer was added to the first one and stored at −80°C until analysis. Before analysis the samples were dried under nitrogen gas at room temperature and reconstituted with acetonitrile.

Quantitative analysis of intracellular ceramides. Liquid chromatography-electrospray ionization tandem-mass spectrometry was used to measure intracellular levels of ceramides C16, C18, C18:1, C20, C22, C24, and C24:1. Ceramide C2 was included as the internal standard. Standards were prepared by dissolving ceramides in a 99.8/0.2 (volume for volume) mixture of ethanol/formic acid to a concentration of 5 mg/mL. Further dilutions were made using acetonitrile to create nine working solutions of 200, 100, 50, 25, 12.5, 6.25, 3.125, 1.56, 0.78, and 0 ng/mL. Standard curves were constructed using linear regression of the peak areas of the analyte versus the corresponding concentrations.

Instrumentation. LC was performed using a Waters Acquity ultraperformance liquid chromatography (UPLC) with a binary pump and Accquity autosampler set at 10°C. Extracted lipids (10 μL) were injected on a Pursuit 3 Diphenyl reversed-phased column (50 × 2.0 mm inner diameter, 3 micron particle column; Varian, Walnut Creek, CA), and flow rate of 0.3 mL/min was applied. The column was at room temperature. The mobile phases were as follows: phase A: 0.1% formic acid and 25 mmol/L ammonium acetate in water; and phase B: 100% acetonitrile. Gradient was 0.10 min B = 30%, 1.10 min B = 95%, 3.00 min B = 95%, and 5.00 min B = 30%. Total run time was 5.00 min. The detector was a Waters Aquity TQD triple quadruple MS/MS with ion source ESI operated in the positive mode. Source and desolvation temperatures were 110°C and 300°C, respectively. The desolvation gas (nitrogen) flow was 600 L/h. No cone gas was used. Collision gas (Argon) flow rate was 0.15 mL/min, and the capillary voltage was 2.47 kV. All ceramides gave the protonated molecular ion $[M+H]^+$ and the same ion after losing a water molecule $[M+H-H_2O]^+$as the major ions and the common product ion 264.2 because the loss of fatty acid and two hydroxyl groups (Supplementary Table 1). According to the retention times of standards, the individual long-chain FFAs were quantified and normalized by protein concentration.

Insulin signaling parameters. Akt-1, Akt-2, and protein tyrosine phosphatase 1B (PTP1B) protein content and phosphorylation were determined by Western blotting as described previously (13,14). Specific antibodies used were anti–Akt-1 and -2, Akt-1 phos (Ser473), Akt-2 phos (Ser474) (Millipore, Temecula, CA), anti-PTP1B and anti-PTP1B phos (Ser50) (ECM Biosciences, Versailles, KY), and β-actin (Santa Cruz Biotechnology, Santa Cruz, CA). In all cases, Western blot results were verified in three separate experiments. To assess the effect of PTP1B expression levels on AKT-1 and -2 phosphorylation, interference RNA (RNAi) was used to downregulate PTP1B expression in FFA and C2-treated cells. Cells in the process of differentiation after 1 day (90–95% confluence) were transfected with 2.5 μg DNA and Lipofectamine 2000 at a ratio of 1:2.5 in 6-well plates in serum-free media. After 6 h, media were switched to that with 2% horse serum for 4 days before treating the cells for 16 h with FFA, ceramide C2 with or without PMI 5011 in serum-free media.

Gene expression. For gene expression, the same treatments above were performed; however, cells were treated for 24 h with 2% horse serum. Total RNA was purified using TRIzol reagent (Invitrogen) according to the manufacturer's instructions. RNA total content and quality was determined spectrophotometrically by absorbance measurements at 260 and 280 nm using the NanoDrop system (NanoDrop Technologies). The cDNAs were synthesized with 2.5 μg of DNA for each sample by reverse transcription (Qiagen) following manufacturer's protocol. Synthesized cDNAs were diluted fourfold. Five microliters of each diluted sample were used for PCR reactions of 20 μL final volume. Other components making up this final volume for PCR reactions were 5 μL of 6 μM gene-specific commercial primers (synthesized by IDT, Coralville, IA) and 10 μL SYBR Green PCR master mix (Qiagen). PCR amplification was carried out by denaturing at 95°C for 15 s, annealing and extension at 60°C for 1 min for 40 cycles. The RT-PCR was analyzed by the Sequence Detection System SDS (Rotor Gene 6000). The amounts of the PTP1B, AKT1, and AKT2 mRNA were normalized to the amount of β-actin mRNA, as an internal control.

PTP1B activity. PTP1B activity was assayed as described previously (14). In brief, the colorimetric *p*-nitrophenyl phosphate (PNPP) hydrolysis assay based on the ability of phosphatases to catalyze the hydrolysis of *p*-nitrophenyl phosphate to *p*-nitrophenol, a chromogenic product, was used. The intensity of the color reaction was measured at 410 nm on a Bio-Rad microplate spectrophotometer. Results were normalized by protein concentration. Experiments were also conducted with and without the presence of a selective inhibitor of PTP1B [3-(3,5-dibromo-4-hydroxy-benzoyl)-2-ethyl-benzofuran-6-sulfonicacid-(4-(thiazol-2-ylsulfamyl)-phenyl)-amide; Calbiochem, Gibbstown, NJ] used at a concentration of 20 μM.

Statistical analysis. All data are presented as means ± SE. Difference between means was determined by ANOVA with subsequent Fisher's protected least significant difference tests or Student's *t* test. $P < 0.05$ was considered significant. All results are an average of three experiments.

RESULTS

Effect of FFA and ceramide exposure on glycogen content. Insulin stimulation resulted in a threefold increase in glycogen content in L6 myotubes when compared with basal conditions (Fig. 1). Incubation with the saturated FFA (i.e., palmitic acid) or ceramide C2 resulted in significantly reduced glycogen content compared with control. Specifically, palmitic acid resulted in a 32% decrease in glycogen content, whereas exposure to C2 resulted in 38.2% and 40.5% decrease at concentrations of 20 ng/mL and 40 ng/mL, respectively (Fig. 1). Incubation with PMI 5011 in the presence of the FFA or C2 resulted in a significant increased glycogen content when compared with incubation of FFA or C2 alone ($P < 0.05$; Fig. 1).

Effect of FFA and PMI 5011 on ceramide formation. Double extraction with methanol/chloroform (1:2) yielded 90.2% recovery for C17, the extraction standard giving assurance of the efficiency of the extraction process. Efficacy of PMI 5011 to reduce ceramide content was compared with that of the fungal toxin myriocin (1 μg/mL), a known inhibitor of serine palmitoyltransferase (SPT), the enzyme that catalyzes the first and rate determining step in the de novo ceramide synthesis process (Fig. 2). Treatment with palmitic acid resulted in a more than twofold increase in all ceramide species. PMI 5011 did not alter total ceramide content when incubated with palmitic acid compared with palmitic acid alone (P = ns). However, myriocin incubation with palmitic acid resulted in ceramide levels that were not different from the control. Ceramide C16 was the most prevalent species formed followed by C24:1. All ceramide species remained elevated in the presence of PMI 5011 and palmitic acid, suggesting that PMI 5011 had no effect of ceramide formation or transformation into metabolites.

Effect of different fatty acids on ceramides and glycogen content. L6 cells incubated with saturated fatty acids (i.e., palmitic [16:0] and stearic [18:0]) resulted in a significant increase in total ceramide content as compared with a nonsignificant increase in ceramide content observed when cells were exposed to the unsaturated fatty acids (palmitoleic [16:1] and oleic acid [C18:1]) (Figs. 3 and 4). Stearic acid (18:0) resulted in a significant increase in ceramide C18 species approximately sevenfold compared with control conditions. Although both stearic (18:0) and oleic (C18:1) acid resulted

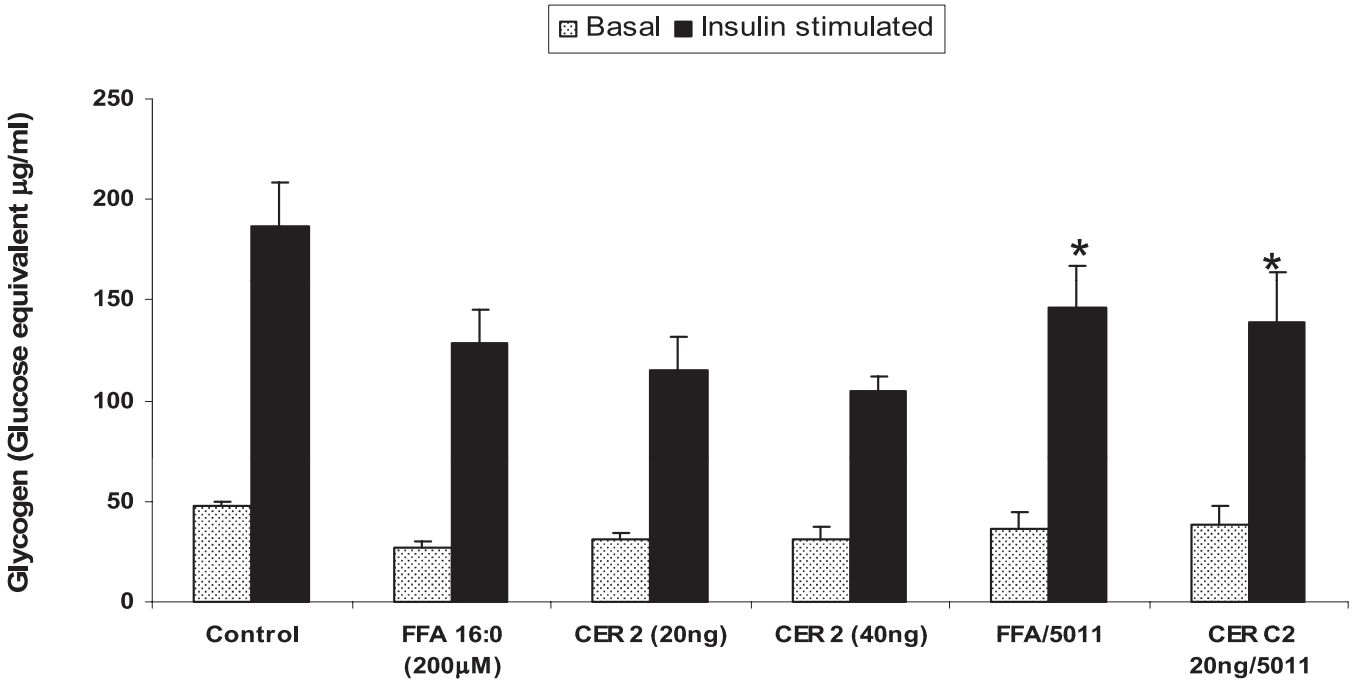

FIG. 1. Glycogen content in both basal and insulin-stimulated states was measured as a marker of insulin action in control cells and in those treated for 24 h with FFA or ceramide (CER) with or without PMI 5011. As shown, glycogen content was significantly reduced with FFA and ceramide C2 incubation. PMI 5011 was observed to mitigate the effect of ceramide C2 and palmitic acid on reducing insulin-stimulated glycogen content. Data are presented as mean ± SEM. *$P < 0.05$ vs. FFA or C2 treatment. All experiments for each condition were conducted in triplicate.

in a threefold increase in the C18:1 ceramide species, the total level of C18:1 was very low (Fig. 3).

The saturated fatty acids palmitic (C16:0) and stearic (C18:0) resulted in significantly reduced glycogen content after insulin stimulation (Fig. 4*A*) and increased total ceramide content (Fig. 4*B*). By contrast, the monosaturated fatty acids, i.e., palmitoleic acid (C16:1) and oleic acid (C18:1), had minimal effect on insulin-stimulated glycogen content and ceramide accumulation (Fig. 4*A* and *B*).

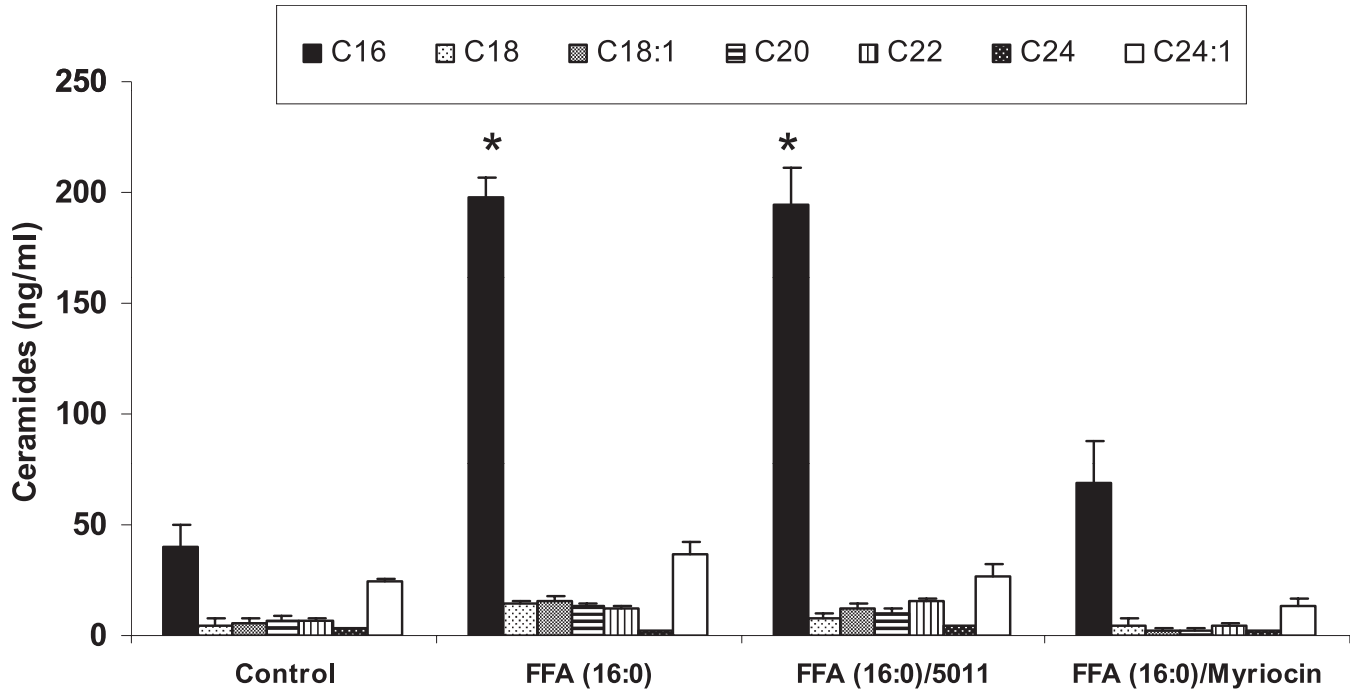

FIG. 2. Effect of PMI 5011 and myriocin on the ceramide profile and total ceramides formed in L6 cells pretreated with palmitic acid as determined by liquid chromatography/tandem mass spectrometry (LCMS/MS). As demonstrated, myriocin significantly inhibited ceramide formation, whereas PMI 5011 had no effect on ceramide formation or accumulation. There was no statistically significant difference in total ceramide levels between FFA-treated cells and those treated with FFA and PMI 5011. Data are presented as mean ± SEM. *$P < 0.05$ vs. control; $n = 3$ assessments for each treatment condition.

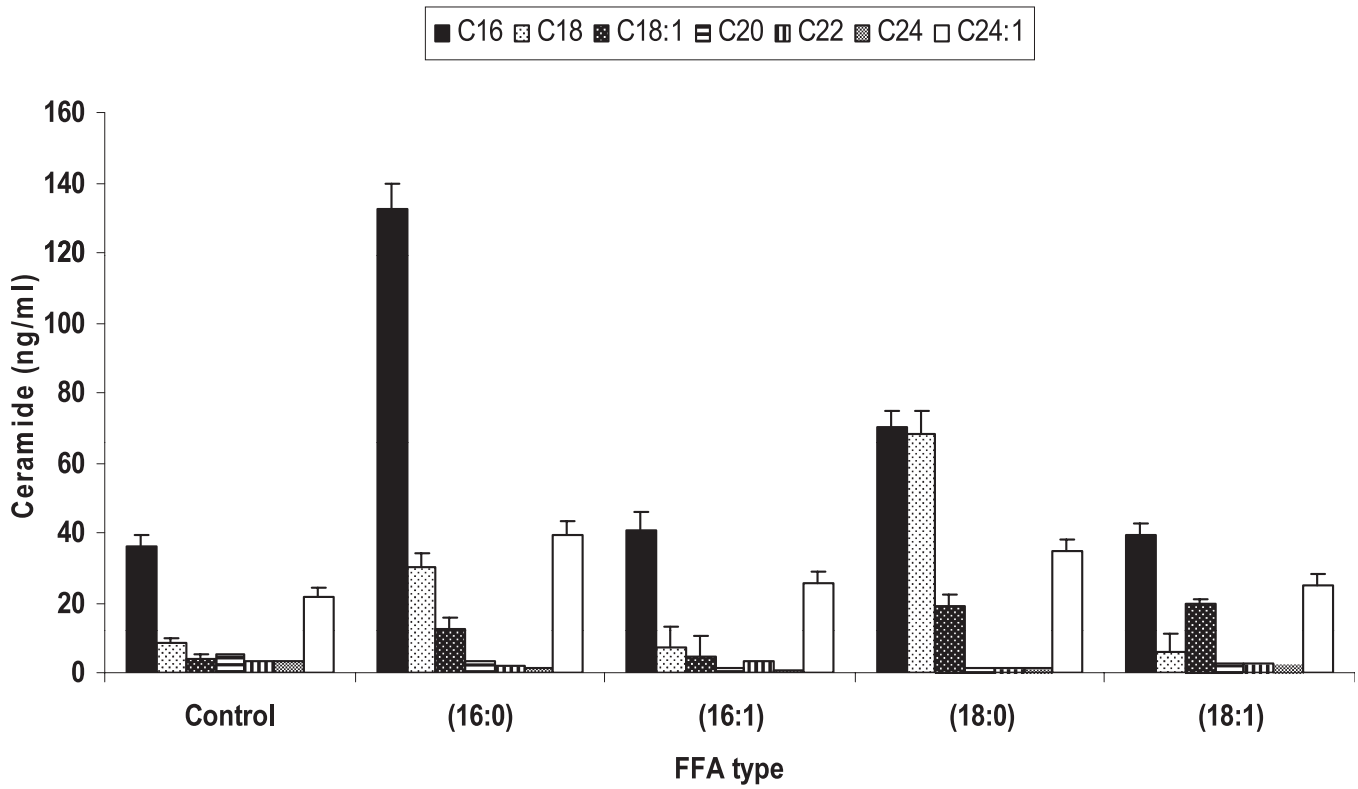

FIG. 3. Ceramide profiles in L6 cells pretreated with different saturated and unsaturated FFAs as determined by liquid chromatography/tandem mass spectrometry (LCMS/MS). C16, C18, and C24:1 were the most prominent ceramide species formed regardless of the FFA treatment used (i.e., C16:0, C16:1, C18:0, and C18:1). Total ceramides as compared with the control treatment increased only in cells treated with saturated FFAs. Unsaturated FFAs had no effect on total ceramide content. n = 3 experiments for each experimental condition.

Effect of ceramide C2 and PMI 5011 on insulin signaling. Incubation of muscle cells with ceramide C2 or palmitic acid significantly blunted insulin-stimulated phosphorylation of both Akt-1 and Akt-2 compared with control conditions (see *lanes 4* and *8* vs. *lane 2*, Fig. 5), and significantly increased PTP1B levels (see *lanes 3* and *4* and *7* and *8* vs. *lanes 1* and *2*). PMI 5011 restored insulin stimulated Akt-1 and -2 phosphorylation in the presence of ceramide or FFA as compared with the ceramide or FFA alone (see *lanes 6* and *10* vs. *lane 4* and *8*, respectively). PMI 5011 reduced PTP1B protein abundance in the presence of ceramide or FFA as compared with the ceramide or FFA alone (see *lanes 5* and *6* and *lanes 9* and *10* vs. *lanes 3* and *4* and *7* and *8*, Fig. 5). Besides reducing PTP1B protein abundance, 5011 also resulted in increased phosphorylation of PTP1B at Ser50 when incubated with C2 or FFA (*lanes 5* and *6* and *lanes 9* and *10*, respectively) when compared with incubation of myotubes with C2 or FFA alone (*lanes 3* and *4* and *lanes 7* and *8*, respectively).

PTP1B activity. Incubation of myotubes with FFAs and ceramide C2 resulted in a significant increase in PTP1B activity compared with that of the control cells (Fig. 6). PMI 5011 significantly reduced PTP1B activity in both FFA-treated and C2-treated cells to levels comparable with those by the PTP1B inhibitor (Fig. 6).

Effect of RNAi to downregulate PTP1B expression. To assess effect of PTP1B expression levels on AKT phosphorylation, we used the use RNAi to downregulate PTP1B expression in FFA-, C2-, and 5011-treated cells. Results showed that when compared with L6 myotubes incubated with FFA or ceramide C2 alone, RNAi lowered PTP1B levels in L6 myotubes incubated with FFA or C2 (see *lanes 9* and *10* vs. *lanes 5* and *6*, Fig. 7*A* and *B*, respectively), and this resulted in increases in insulin stimulated AKT1 and AKT2 phosphorylation (see *lane 10* vs. *lane 6*, Fig. 7*A* and *B*). Addition of PMI 5011 to cells treated with FFA or C2 appeared to have greater effects on Akt-1 and Akt-2 phosphorylation as compared with transfected cells treated with FFA or C2 (see *lanes 8* vs. *10*, Fig. 7*A* and *B*). It is noteworthy that PMI 5011 was noted again to have effects to enhance PTP1B phosphorylation when either treated with FFA or C2 alone or in transfected cells treated with FFA or C2 (see *lanes 8* and *12* vs. *lanes 6* and *10*, Fig. 7*A* and *B*, respectively).

Gene expression revealed that both FFA and ceramide C2 significantly increased PTP1B mRNA expression (Fig. 8*A* and *B*). Use of RNAi or PMI 5011 separately as intervention reduced PTP1B expression to levels not different from those of control. AKT1 and AKT2 expression remained unchanged after intervention (Fig. 8*A* and *B*).

DISCUSSION

Our data demonstrate that pretreatment of myotubes with saturated FFAs mirrors the effect of clinical metabolic dysregulation because this intervention attenuated insulin signaling and resulted in blunted insulin action. Specifically, we noted a reduction in both Akt-1 and Akt-2 phosphorylation and reduced insulin-stimulated glycogen content with exposure to saturated FFAs. In agreement with other reports (2,3), we demonstrated a consistent increase in lipid metabolites, i.e., ceramide content, with FFA incubation and that ceramide C2, a cell-permeable

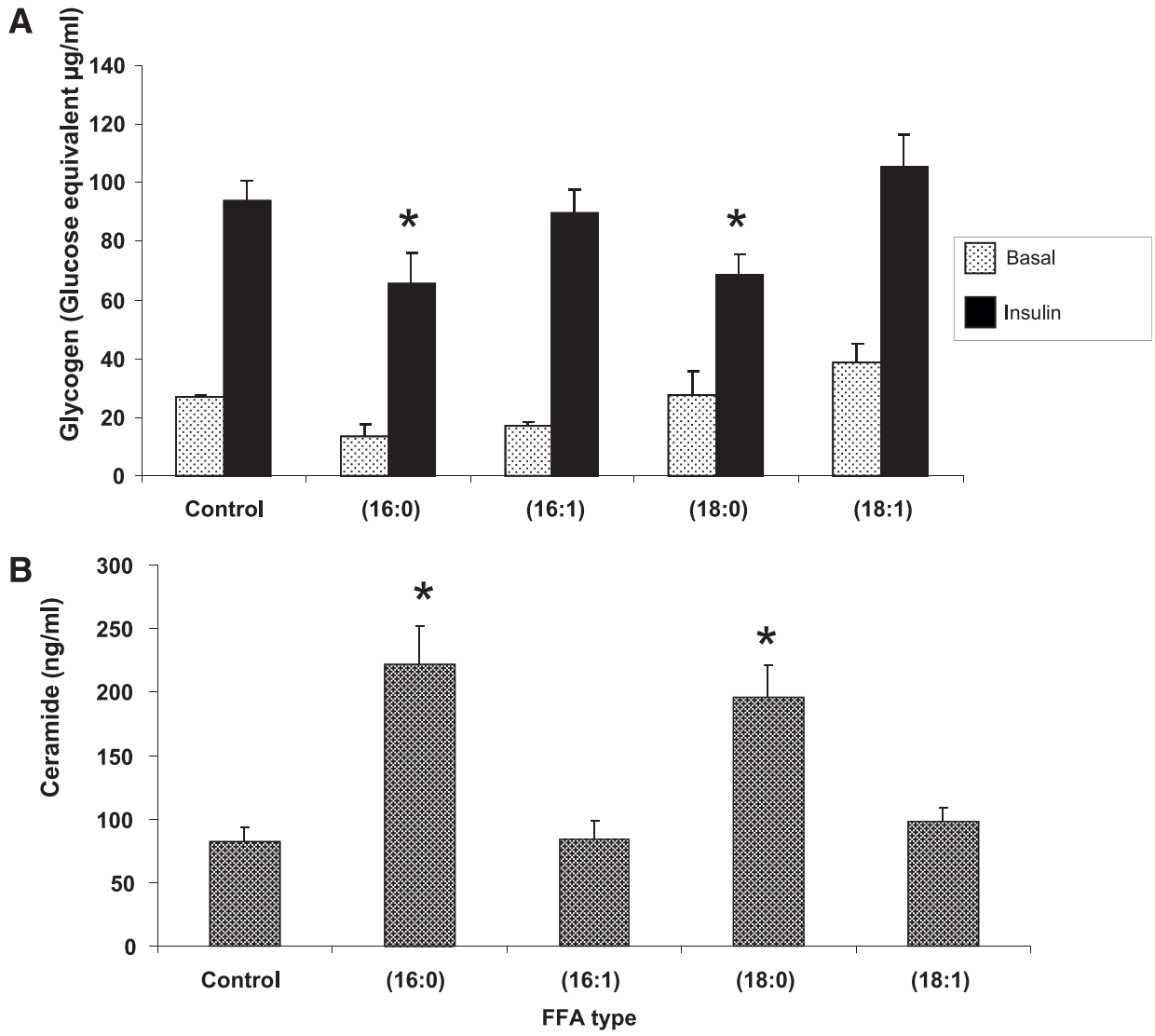

FIG. 4. Demonstration of a comparison of effect of FFA type on glycogen content (*A*) and total ceramides formed (*B*) in L6 cells. *A*: Glycogen content was used as a marker of insulin sensitivity in cells treated with FFAs for 24 h. *B*: Another set of cells also treated for 24 h was used to measure total ceramides by liquid chromatography/tandem mass spectrometry (LCMS/MS) after extraction of the lipid fraction by methanol/chloroform partition. As demonstrated, palmitic acid and stearic acid were significantly different from the control for both total ceramides and glycogen content. Elevated ceramide levels were associated with significantly lower glycogen content. *$P < 0.05$ vs. control; $n = 3$ experiments for each treatment condition.

analog of the long-chain ceramides, closely replicated the effects of the saturated FFAs. We report that the mechanism by which PMI 5011 improves insulin action was not secondary to an effect on the formation or accumulation of ceramides. However, novel information was obtained suggesting that the botanical reverses the effect of intramuscular-formed ceramides on Akt phosphorylation and hence modulated their role in insulin signaling in L6 cells.

Ceramides with different compositions are produced by de novo synthesis via condensation of palmitoyl-CoA and Ser (4) or activation of sphingomyelinases under physiological stress (7). In the presence of excess FFAs, long-chain fatty acyl-CoAs derived from the FFAs are diverted away from carnitine palmitoyltransferase 1, the mitochondrial enzyme that catalyzes the first step in β-oxidation, and are instead preferentially partitioned toward the synthesis of signaling intermediates diacylglycerol, triglycerides, and ceramides. We confirmed this pathway by preincubation of cells with different FFAs and observed distinct effects on insulin sensitivity and accumulation of both total ceramides generated and specific ceramide species. The rate-limiting reaction in ceramide synthesis is the SPT catalyzed condensation of Ser with palmitoyl-CoA. Myriocin, an inhibitor of SPT, inhibited accumulation of ceramides demonstrating the involvement of the de novo pathway. Palmitate provides the precursor palmitoyl-CoA and/or induces SPT expression (2,4). Unsaturated palmitoleic (16:1) and oleate (18:1) did not result in a significant increase in total ceramides and had no effect on the ceramide profile because SPT is highly specific to saturated FFAs with 16 ± 1 carbon atoms (4). The incorporation of the second fatty acyl-CoA during the conversion of sphinganine into dihydroceramide uses both unsaturated and saturated FFAs. Oleate caused an increase in the corresponding ceramide C18:1 almost fivefold, confirming its involvement in this step. However, total levels of C18:1 were too low compared with those of

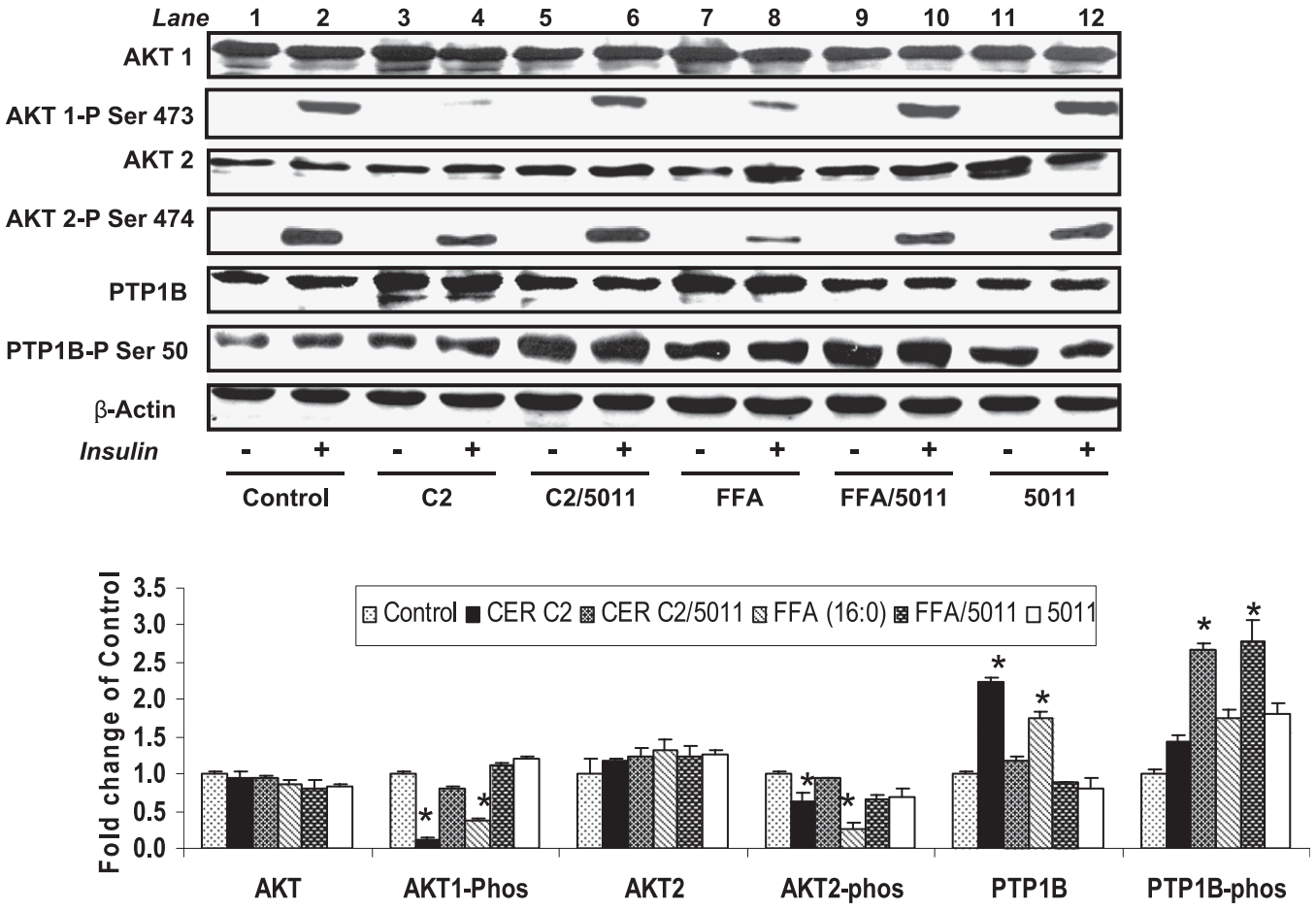

FIG. 5. Effect of FFA, ceramide (CER), and PMI 5011 on Akt-1, Akt-2, and PTP1B expression and phosphorylation (phos). L6 cells were pretreated with palmitic acid (200 μM) or ceramide C2 (20 ng/mL) for 16 h before insulin stimulation. The bar graphs summarize the results of quantification of gel plots from three experiments. *$P < 0.05$ indicates a significant difference for each parameter compared with the control. As shown, palmitic acid and ceramide C2 attenuated the increase in phosphorylation of Akt-1 and -2 postinsulin stimulation. PMI 5011 incubation with either C2 or with FFA restored AKT1 phosphorylation and downregulated PTP1B expression compared with incubation with either C2 or FFA alone (see *lanes 5* and *6* vs. *lanes 3* and *4*, and *lanes 9* and *10* vs. *lanes 8* and *9*). Increased Akt-1 and Akt-2 phosphorylation resulted in increased PTP1B phosphorylation.

C16, C18, and C24:1. Our observations demonstrated that the saturated FFAs palmitic (16:0) and stearic (18:0) reduced glycogen content, and this was associated with increased ceramide levels. In contrast, palmitoleic (16:1) and oleic (18:1), which caused minimal ceramide increase, resulted in no net effect on glycogen content, confirming the importance of ceramides as a metabolite linking lipid oversupply to the antagonism of insulin signaling. The observation is consistent with dietary studies indicating that saturated fats markedly decrease insulin responsiveness in peripheral tissues, whereas unsaturated fats may have weaker or in some cases insulin-sensitizing effects (2). Our findings correlate with those of Ghosh et al. (5) who showed that the proinflammatory cytokine tumor necrosis factor-α (TNF-α) activates both de novo and hydrolysis pathways of ceramide generation. In their study, L6 cells assayed for ceramide content also showed that C16 and C24:1 ceramides were the predominant species detected after TNF-α treatment.

Clinical interventions, i.e., thiazolidinediones and exercise, which reduce cellular lipids, have been reported to increase insulin action (4,8,9,17). Stearoyl-CoA desaturase, a microsomal enzyme, catalyzes the synthesis of monounsaturated fatty acids from saturated fatty acyl-CoAs and plays a key role in the synthesis of triglycerides, cholesteryl esters, and membrane phospholipids. Dobrzyn et al. (18) reported that depletion of stearoyl-CoA desaturase lowers ceramide levels and improves insulin sensitivity. Because PMI 5011 has been shown to significantly increase glucose uptake and partially restore glycogen accumulation (13,14), we hypothesized that the insulin-sensitizing effects of PMI 5011 may be secondary to reducing the accumulation of ceramides observed in the presence of increasing FFA concentrations. However, all seven ceramide species remained elevated in the presence of PMI 5011. We therefore concluded that the mechanism by which PMI 5011 restores insulin signaling is not through preventing accumulation of ceramides. This study did not, however, rule out the fact that 5011 may have some effects on downstream metabolism of the ceramides into forms that are less deleterious to insulin signaling, while still maintaining high overall ceramide levels. Specifically, ceramides can be metabolized to less toxic forms by the addition of a phosphorylcholine group to form sphingomyelin. They can also be deacylated (by ceramidases), phosphorylated (by ceramide kinase), or glycosylated (by glucosylceramide synthase) resulting in molecules that may have a less deleterious effect on insulin signaling (4,17). Overexpression of acid ceramidase has been shown to prevent palmitate-induced insulin resistance in C2C12

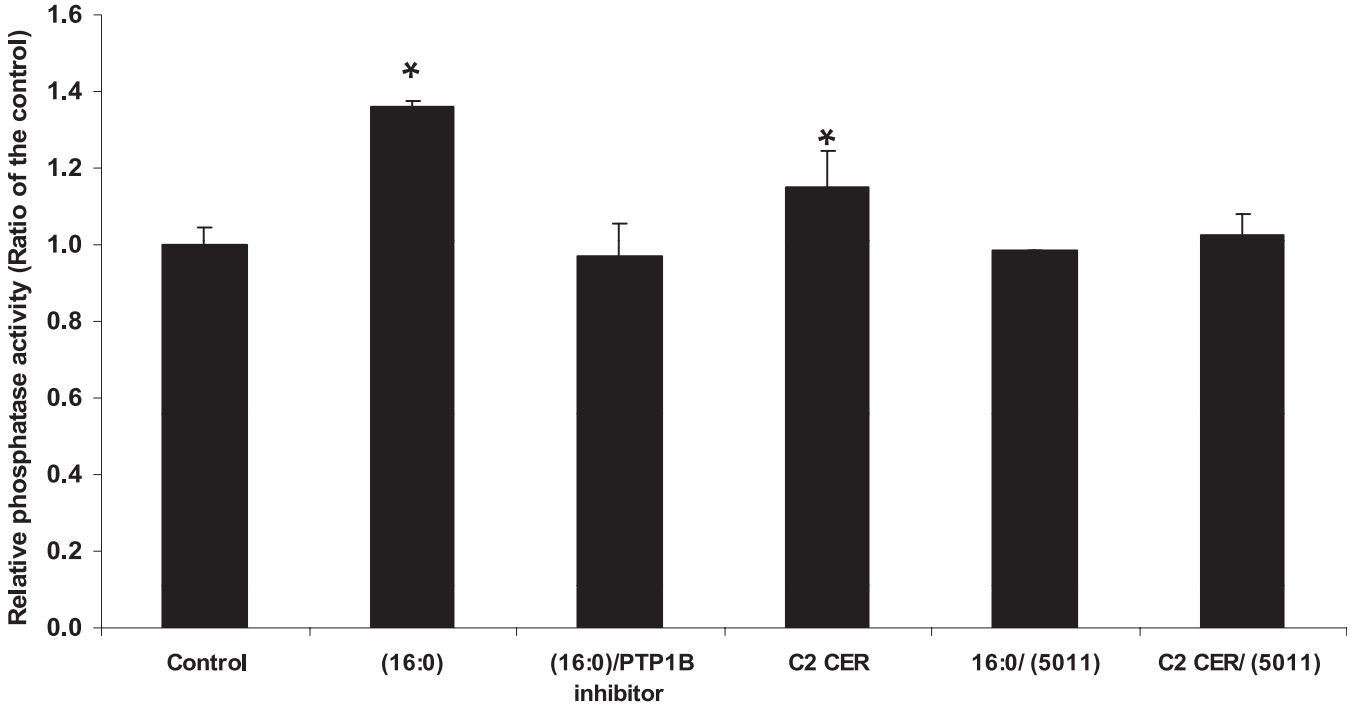

FIG. 6. Effect of pretreatment with fatty acids and ceramide (CER) on PTP1B activity in L6 cells. Cells were treated with 200 μM palmitic acid or 20 ng/mL C2 with or without PMI 5011 for 24 h. For comparison, cells were also incubated in the presence of an inhibitor of PTP1B. Palmitic acid and C2 significantly increased PTP1B activity. PMI 5011 was observed to significantly reduce PTP1B activity in the presence of FFA or ceramide (C2) exposure. *$P < 0.05$ vs. control; $n = 3$ experiments for each treatment condition.

muscle cells (19). Thus the study did not rule out whether PMI 5011 promotes any of these metabolism processes.

Consistent with the reports of Chavez and Summers (2), Schmitz-Peiffer et al. (19), and Bourbon et al. (20), ceramide C2 inhibited insulin-stimulated phosphorylation of PKB/Akt. Ghosh et al. (5) also showed that ceramide C6 mimicked the effects of TNF-α in attenuating insulin signaling by reducing AKT phosphorylation at Ser473. However, our study showed that PMI 5011 significantly enhanced insulin sensitivity by restoring PKB/Akt phosphorylation even in the presence of elevated FFA or ceramide levels. Akt activation is dependent on its phosphorylation at two key residues: Thr308 and Ser473/474. In particular, phosphorylation at Ser473 and Ser474 is necessary for the full activation of Akt kinase activity. Reduced insulin-stimulated Akt is evident in insulin-resistant obese individuals. Akt/PKB promotes the uptake of lipids and amino acids in various tissues and regulates a variety of intracellular enzymes that promote the incorporation of nutrients into glycogen, protein, and triacylglycerol including glycogen synthase kinase 3b (GSK3b), an upstream inhibitor of glycogen synthesis. Thus the reduction of glycogen content observed with pretreatment with the saturated fatty acids and ceramide C2 may stem from the inhibition of Akt/PKB phosphorylation and hence attenuation of its role in the insulin signaling pathway.

Besides inhibiting Akt phosphorylation, ceramide C2 increased the expression and activity of PTP1B, an abundant PTPase within skeletal muscle and a therapeutic target for type 2 diabetes. Increased PTP1B protein content was consistent with elevated PTP1B phosphatase activities (Fig. 6). Increased activity of phosphatases can be one of the mechanisms inhibiting the insulin signaling pathway (21). PTP1B dephosphorylates the insulin receptor and insulin receptor substrate. A study by Ravichandran et al. (22) showed that PTP1B can function as a substrate for Akt in cells. They demonstrated that phosphorylation of PTP1B by Akt at Ser50 negatively modulates its phosphatase activity, creating a positive feedback mechanism for insulin signaling by impairing its ability to dephosphorylate the insulin receptor. Testing for PTP1B phosphorylation showed that it increased when AKT phosphorylation increased with 5011 (Fig. 5). When Akt is inactivated by reduced phosphorylation by ceramides in this case, its negative modulation of PTP1B is reduced. It is noteworthy that PMI 5011 treatment consistently resulted in much higher levels of PTP1B phosphorylation. Thus, in this study, PMI 5011 was demonstrated to have three specific and possibly interrelated effects on the insulin signaling pathway. First, it restored Akt phosphorylation. Second, it increased phosphorylation of PTP1B, hence negatively modulating PTP1B activity in dephosphorylating the insulin receptor. It was not concluded as to whether this was a direct effect or secondary to the enhanced Akt phosphorylation. Finally, PMI 5011 decreased PTP1B protein expression in FFA and in ceramide C2–pretreated cells. A decrease in PTP1B or its phosphorylation improves insulin action by reducing its capacity to dephosphorylate the insulin receptor thus improving insulin resistance (22). Overall, the net sum of the effects of PMI 5011 was to lower PTP1B activity to a level comparable to that observed of the specific PTP1B inhibitor in both palmitate and C2 pretreated cells.

Conclusions. Our data demonstrate that the mechanism by which PMI 5011 modulates insulin action in metabolically dysregulated states is not secondary to an effect on ceramide formation and accumulation. With PMI 5011 intervention, we observed increased insulin signaling via restoration of insulin-stimulated Akt-1 and Akt-2 phosphorylation despite presence of high ceramide levels in cells. PMI 5011

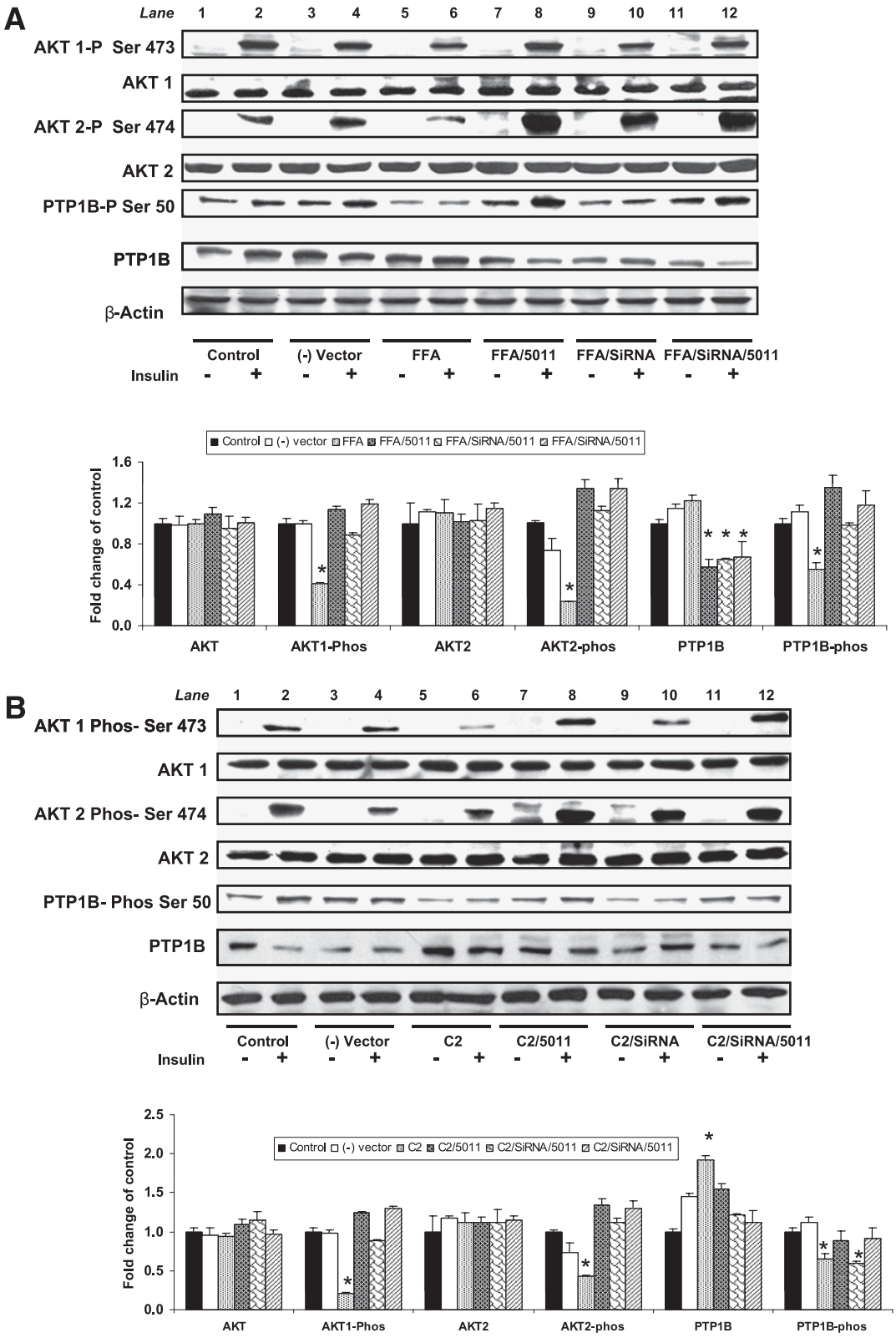

FIG. 7. ***A*** **and** ***B*****: Demonstration of use of RNAi to downregulate PTP1B expression in FFA and C2-treated cells. L6 control and transfected cells were pretreated with palmitic acid (200 μM) or ceramide C2 (20 ng/mL) for 16 h before insulin stimulation (10 nmol/L for 10 min). Akt-1, Akt-2, PTP1B levels, and phosphorylation were assessed. The bar graphs summarize the results of quantification of gel plots from three experiments. When compared with the negative vector, use of RNAi reduced PTP1B levels in L6 cells treated with C2 and FFA only (*** *lanes 5* **and** *6* **vs.** *lanes 9* **and** *10*** **). Use of small interfering RNA (SiRNA) in the presence of C2 and FFA treatment increased insulin-stimulated Akt-1 and Akt-2 phosphorylation modestly compared with the C2 and FFA treatment (*** *lanes 9* **and** *10* **vs.** *lanes 5* **and** *6*** **). Data are means ± SEM. *$P < 0.05$ indicates a significant difference compared with the control.**

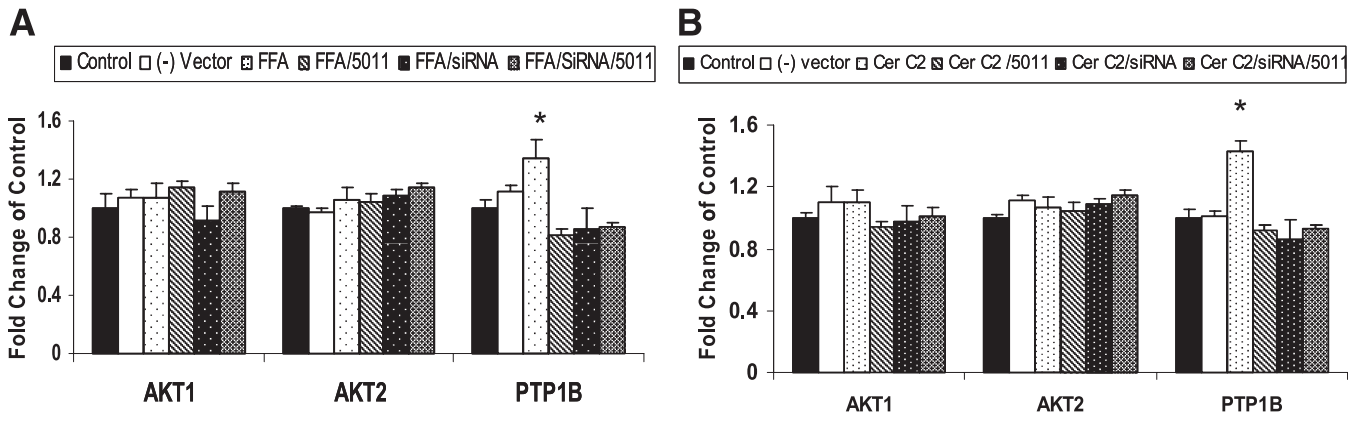

FIG. 8. ***A*** **and** ***B*****: AKT 1, AKT 2, and PTP1B gene expression shown as fold induction compared with the control. The effects of 200 μM palmitic acid and 20 ng ceramide (Cer) C2 with or without PMI 5011 on mRNA expression in differentiated L6 cells were determined. As shown, both FFA and ceramide C2 increased PTP1B, but not Akt-1 or -2 gene expression. RNAi and PMI 5011 reduced PTP1B gene expression in the presence of FFA or ceramide C2. Data are means ± SEM. *$P < 0.01$ vs. control; $n = 3$ experiments for each treatment condition. siRNA, small interfering RNA.**

mitigated the upregulation of PTP1B that is observed in the presence of excess FFA or ceramide accumulation. It is noteworthy that PMI 5011 was noted to consistently enhance PTP1B phosphorylation and, as such, reduce its phosphatase activity against intracellular substrates of insulin signaling, thus providing a novel observation regarding its mechanism of action.

ACKNOWLEDGMENTS

This work was supported by P50AT002776-01 from the National Center for Complementary and Alternative Medicine and the Office of Dietary Supplements, which funds the Botanical Research Center of Pennington Biomedical Research Center and the Biotech Center of Rutgers University.

No potential conflicts of interest relevant to this article were reported.

D.N.O. and W.T.C. designed the studies, reviewed and analyzed the data, and wrote the manuscript. D.N.O., A.H., Y.Y., X.H.Z., and Z.Q.W. conducted research studies and reviewed and edited the manuscript. D.R. prepared the plant material from growth, extraction, and purification of the extract. W.T.C. is the guarantor of this work and, as such, had full access to all the data in the study and takes responsibility for the integrity of the data and the accuracy of the data analysis.

Parts of this study were presented in abstract form at the 71st Scientific Sessions of the American Diabetes Association, San Diego, California, 24–28 June 2011.

REFERENCES

1. Koves TR, Ussher JR, Noland RC, et al. Mitochondrial overload and incomplete fatty acid oxidation contribute to skeletal muscle insulin resistance. Cell Metab 2008;7:45–56
2. Chavez JA, Summers SA. Characterizing the effects of saturated fatty acids on insulin signaling and ceramide and diacylglycerol accumulation in 3T3-L1 adipocytes and C2C12 myotubes. Arch Biochem Biophys 2003;419:101–109
3. Chavez JA, Knotts TA, Wang LP, et al. A role for ceramide, but not diacylglycerol, in the antagonism of insulin signal transduction by saturated fatty acids. J Biol Chem 2003;278:10297–10303
4. Summers SA. Ceramides in insulin resistance and lipotoxicity. Prog Lipid Res 2006;45:42–72
5. Ghosh N, Patel N, Jiang K, et al. Ceramide-activated protein phosphatase involvement in insulin resistance via Akt, serine/arginine-rich protein 40, and ribonucleic acid splicing in L6 skeletal muscle cells. Endocrinology 2007;148:1359–1366
6. Guenther GG, Peralta ER, Rosales KR, Wong SY, Siskind LJ, Edinger AL. Ceramide starves cells to death by downregulating nutrient transporter proteins. Proc Natl Acad Sci USA 2008;105:17402–17407
7. Reynolds CP, Maurer BJ, Kolesnick RN. Ceramide synthesis and metabolism as a target for cancer therapy. Cancer Lett 2004;206:169–180
8. Dobrzyń A, Górski J. Ceramides and sphingomyelins in skeletal muscles of the rat: content and composition. Effect of prolonged exercise. Am J Physiol Endocrinol Metab 2002;282:E277–E285
9. Helge JW, Dobrzyn A, Saltin B, Gorski J. Exercise and training effects on ceramide metabolism in human skeletal muscle. Exp Physiol 2004;89:119–127
10. Planavila A, Alegret M, Sánchez RM, Rodríguez-Calvo R, Laguna JC, Vázquez-Carrera M. Increased Akt protein expression is associated with decreased ceramide content in skeletal muscle of troglitazone-treated mice. Biochem Pharmacol 2005;69:1195–1204
11. Ribnicky DM, Poulev A, Watford M, Cefalu WT, Raskin I. Antihyperglycemic activity of Tarralin, an ethanolic extract of *Artemisia dracunculus L.* Phytomedicine 2006;13:550–557
12. Ribnicky DM, Kuhn P, Poulev A, et al. Improved absorption and bioactivity of active compounds from an anti-diabetic extract of *Artemisia dracunculus L.* Int J Pharm 2009;370:87–92
13. Wang ZQ, Ribnicky D, Zhang XH, Raskin I, Yu Y, Cefalu WT. Bioactives of *Artemisia dracunculus L* enhance cellular insulin signaling in primary human skeletal muscle culture. Metabolism 2008;57(Suppl. 1):S58–S64
14. Wang ZQ, Ribnicky D, Zhang XH, et al. An Extract of *Artemisia dracunculus L.* enhances insulin receptor signalling and modulates gene expression in skeletal muscle in KKa^{y} mice. J Nutr Biochem. In press
15. Gómez-Lechón MJ, Ponsoda X, Castell JV. A microassay for measuring glycogen in 96-well-cultured cells. Anal Biochem 1996;236:296–301
16. Haynes TA, Duerksen-Hughes PJ, Filippova M, Filippov V, Zhang K. C18 ceramide analysis in mammalian cells employing reversed-phase high-performance liquid chromatography tandem mass spectrometry. Anal Biochem 2008;378:80–86
17. Merrill AH Jr. De novo sphingolipid biosynthesis: a necessary, but dangerous, pathway. J Biol Chem 2002;277:25843–25846
18. Dobrzyn A, Dobrzyn P, Lee SH, et al. Stearoyl-CoA desaturase-1 deficiency reduces ceramide synthesis by downregulating serine palmitoyltransferase and increasing beta-oxidation in skeletal muscle. Am J Physiol Endocrinol Metab 2005;288:E599–E607
19. Schmitz-Peiffer C, Craig DL, Biden TJ. Ceramide generation is sufficient to account for the inhibition of the insulin-stimulated PKB pathway in C2C12 skeletal muscle cells pretreated with palmitate. J Biol Chem 1999;274:24202–24210
20. Bourbon NA, Sandirasegarane L, Kester M. Ceramide-induced inhibition of Akt is mediated through protein kinase Cζ: implications for growth arrest. J Biol Chem 2001;277:3286–3292
21. Taghvaei NM, Meshkani R, Taghikhani M, Larijani B, Adeli K. Palmitate enhances protein tyrosine phosphatase 1B (PTP1B) gene expression at transcriptional level in C2C12 skeletal muscle cells. Inflammation 2011;34:43–48
22. Ravichandran LV, Chen H, Li Y, Quon MJ. Phosphorylation of PTP1B at Ser (50) by Akt impairs its ability to dephosphorylate the insulin receptor. Mol Endocrinol 2001;15:1768–1780